Technical Document

Partial Discharge Pulse Shape Analysis to Discriminate Near and Far End Failures for Cable Location

P. Treyer, P. Mraz, U. Hammer

TD-106

HAEFELY

Current and voltage – our passion

PARTIAL DISCHARGE PULSE SHAPE ANALYSIS TO DISCRIMINATE NEAR AND FAR END FAILURES FOR CABLE TESTING

Patrick Treyer[1*], Petr Mraz[1] and Urs Hammer[1]
[1]Haefely Hipotronics, Birsstrasse 300, 4052 Basel, Switzerland
*Email: <treyer.patrick@haefely.com>

Abstract: Apparent charge measurement according to IEC 60270 is performed during high-voltage cable routine test. In case the partial discharge (PD) level exceeds the specified acceptance limits, PD cable site location functionality enables the operator to locate the position of the failure. Due to various types of cable construction, different insulating materials and insulation wall thicknesses, and variable background noise levels it is difficult to determine an absolute value for the required accuracy of PD site location. However, experience has shown that an accuracy of 1% of the full cable length is achievable. Using commercially available PD site location analyzing systems it is more difficult or even impossible to locate faults closer than 20 meters from the cable far end. This issue is caused by pulse superposition resulting from the limited PD bandwidth of the test arrangement. An increase of the PD measurement bandwidth will lead to augmented noise levels and sensitivity to high-voltage connection lengths and local reflections.

In this paper, the theory of PD site location on high-voltage cables is described and discussed. We present a novel approach for site location enabling the user to accurately discriminate between near and far end cable faults. The method is based on the recording and comparison of pulse widths and shapes at the time of calibration and during measurement in order to determine whether the failure is located at the near or far end of the cable. The influence of the coupling capacitor, cable termination and coupling impedance is assessed to provide recommendations for a successful test setup.

1   INTRODUCTION

This paper revisits the theory related to cable fault location, investigates near/far end calibration characteristics and explores optimizations of the test setup and pulse processing using techniques such as matched filtering, derivative or auto-correlation for pulse width measurement. The paper concludes by an example and method to discriminate near and far end failures. Rather than finding an accurate model of a particular setup the purpose of this work is to propose a method that can be directly exploited in most situations.

2   THEORY

Cable fault location mainly consists of measuring the time between partial discharge pulses. This section covers the basic theory to characterize the relevant parameters for faults located close to the cable ends.

2.1   Bandwidth and Pulse Separation

The Nyquist theorem defines the main relationship between bandwidth (BW) and the maximum pulse rate which can be transmitted on a cable. The most well-known application of this theorem is the Nyquist filter, a digital filter used to transmit data in a limited BW reaching the theoretical limit of Equation 1. This limit applies as well to pulses that can be separated and detected in PD site location applications without (positive) superposition.

$$PRF = 2 \cdot BW \tag{1}$$

where:

BW = available BW in Hertz (Hz)
PRF = Pulse repetition frequency in Hertz

The optimum BW in time domain PD measurement for distribution cables is up to 20 MHz (but can be less depending on the cable length) which allows to separate pulses as close as 25 ns resulting in a spatial resolution of. 2.5 m [1,2,3]. Increased cable attenuation at higher frequencies as well as the influence of the coupling capacitor are the main limiting factors. PD pulses are generated in short burst sequences after each PD event, which leads to the possibility of using the pulse width to further detect superimposed pulses.

2.2   Sampling Rate and Time Resolution

The sampling rate of the analog-to-digital converter (ADC) is the basic parameter defining the time resolution of the measuring system but the ultimate boundary for the time resolution is limited by the ADC sample and hold aperture jitter as well as ADC clock jitter and linearity. By means of signal processing the time and amplitude resolution can be increased to the limit determined by these additional parameters. An increase of the resolution by a factor of ten or more can be easily achieved.

2.3 Cable Characteristic Impedance and Reflection Coefficient

The cable characteristic impedance can be either calculated from the insulation characteristics and the conductor sizes or from two impedance measurements with a short circuit and open termination of the cable [4].

$$Z_o(f) = \sqrt{Z_{open}(f) \cdot Z_{short}(f)} \qquad (2)$$

where:

f = frequency (Hz)
Z_o = characteristic impedance Ω
Z_{open} = open end cable impedance in Ω
Z_{short} = shorted end cable impedance in Ω

The reflection coefficient is given as follows [4]:

$$\Gamma = \frac{Z_L - Z_o}{Z_L + Z_o} = \frac{E_{refl}}{E_{inc}} \qquad (3)$$

where:

Γ = reflection coefficient
Z_L = load impedance in Ω
E_{refl} = reflected voltage wave
E_{inc} = incident voltage wave

2.4 Near and Far End Pulse Patterns

Depending on the PD event location the recorded pulse sequence starts with a single isolated pulse or a pair of pulses.
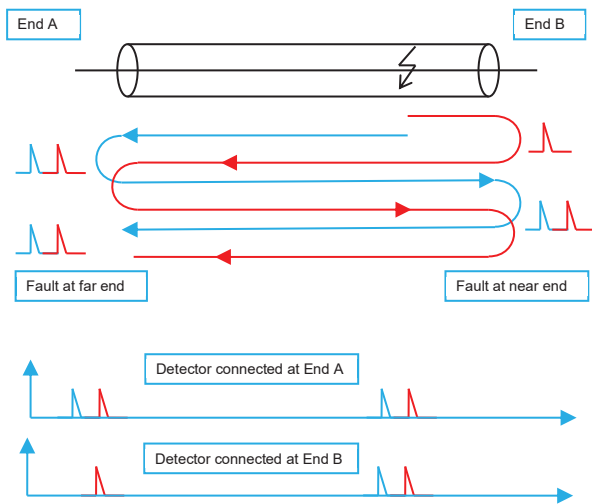

Figure 1: Near end vs. far end pulse patterns.

The subsequent pulses always appear as a pair of pulses. The time between the two pulses of a pair of pulses is proportional to the distance of the fault from the cable end.

When the fault is close to one of the cable ends the pair of pulses appears as a single pulse due to superposition.

3 CALIBRATION

3.1 Calibration Pulse in Frequency Domain

The test object C_a according to IEC 60270 is supposed to be capacitive or to behave as a capacitor which is mostly the case for small test objects. However, the test object can also behave as a pure inductor [5] or as an LC network [6] - both cases allow equally valid calibration according to IEC 60270.

In case of high-voltage cables the test object mostly behaves as an ideal resistor. This leads to a calibration pulse spectrum with lower cut-off frequency as per Equation 4.

$$F_{low}(-6dB) = \frac{1}{2 \cdot \pi \cdot \sqrt{3} \cdot (R_M + Z_o) \cdot C_k} \qquad (4)$$

where:

F_{low} = lower cut off frequency (Hz)
R_M = measuring impedance (Ω)
Z_o = cable characteristic impedance (Ω)
C_k = coupling capacitance (F)

Figure 2 shows the schematic of a cable with 5 µs transmission delay which is terminated with its characteristic impedance of 30 Ω to avoid reflections. The calibrator model is an ideal swept current generator according to the method described in [5].
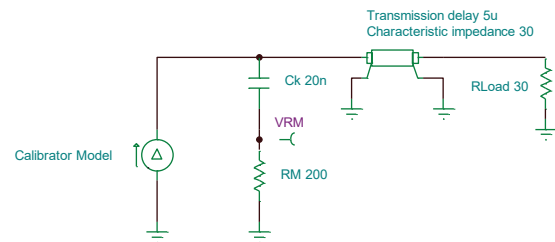

Figure 2: Calibration setup.

This simple setup is used to confirm the flat pulse spectrum which is the first requirement to validate the calibration principle.

3.2 Calibration Pulse in Time Domain

For the time domain, an ideal step generator V_i combined with an ideal capacitor C_i was used for simulation.
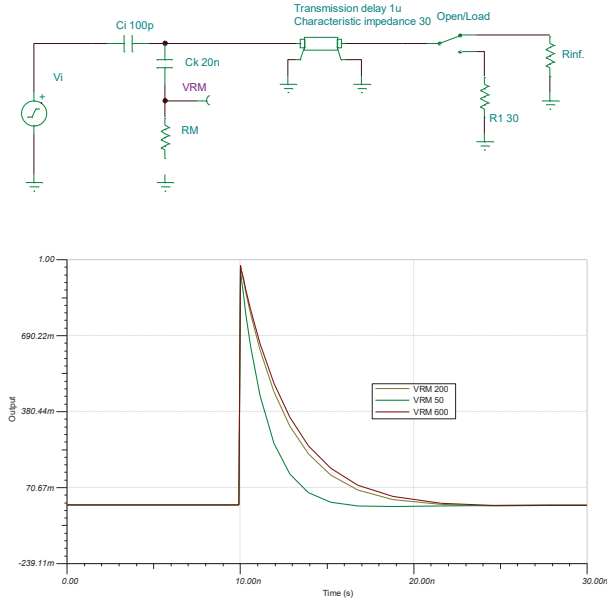
Figure 3: Time domain signal of the calibration pulse.

Provided that $C_i << C_k$

$$q = C_i \cdot V_i \qquad \text{and} \qquad R_{eq} = \frac{R_a \cdot R_M}{R_a + R_M} \qquad (5)$$

$$V_{RM}(t) = V_i \cdot e^{\frac{-t}{R_{eq} \cdot C_i}} \qquad (6)$$

$$Q_m = \frac{1}{R_M} \int_0^\infty V_{RM}(t) \cdot dt = \frac{R_a}{R_a + R_M} \cdot q \qquad (7)$$

With Q_m proportional to the injected charge q, the second requirement to validate the calibration principle is fulfilled. Here, no C_i/C_a requirements apply as for pure capacitive test objects since the cable behaves as a resistive load – transmission line. In the case of cable test objects the important requirement is to keep C_i small enough to avoid any variations of the reflection coefficient between calibration and measurement as well as to keep the BW of the calibration pulse higher than the system BW.

3.3   Near and Far End Calibration

The circuit simulations shown in Figure 4 compare the pulse shape and magnitude for near end and far end calibration as well as for a PD event along the cable. The diagram shows both full bandwidth PD pulses (Far, Near, PD Event) and also 20 MHz low-pass (LP) filtered signals (FiltFar, FiltNear, FiltPDevent) which reveals the fact that the near end calibration pulse has the same charge magnitude as the PD event along the cable. On the other hand, the far end calibration pulse exhibits twice the magnitude (in fact the LP filter results in an integration of the pulse waveform hence reflecting the PD level).
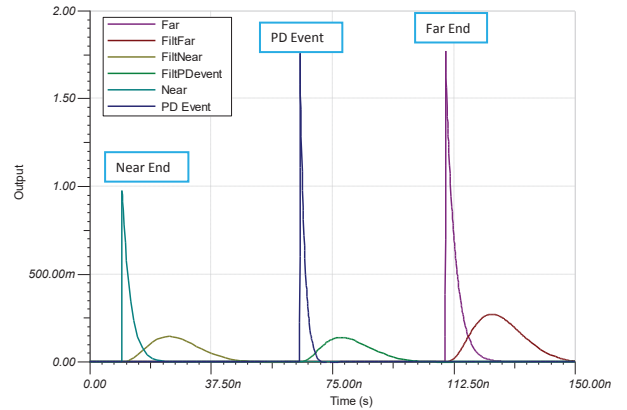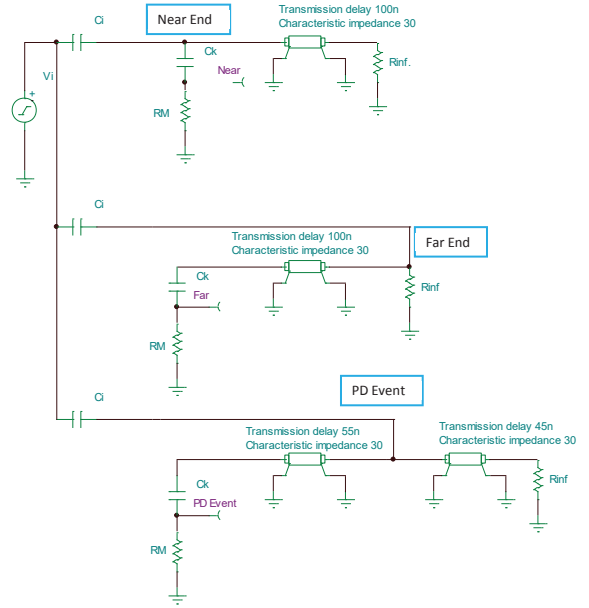

Figure 4: Near end vs. far end calibration.

The PD event signal is always measured equally by the PD detector. However, a difference is observed in the calibration factor which changes by a factor of two when calibrating at the near or far end. In the case of far end calibration, the full charge is entering the cable. In case of the PD event the charge is split into two pulses both carrying half of the full charge. The near end pulse has a magnitude of V_i (PD Calibrator) whereas the far end and PD event pulses have a magnitude of $2*V_i$ because of the reflection coefficient at the near end. The near end calibration signal is proportional to R_{eq}/Z_o while the far end calibration is proportional to $1+\Gamma$. Since

$$2 \cdot \frac{R_{eq}}{Z_o} = 1 + \Gamma \qquad (8)$$

the charge reading for near end and far end calibration differs by a factor of two. Table 1 summarizes the calibration and measurement parameters when calibrating at the cable near or far end.

Table 1: Near and far end calibration parameters.

Parameter	Near End	Far End
$V_{cal}(t)$	$V_i \cdot e^{\frac{-t}{R_{eq} \cdot C_i}}$	$V_i \cdot e^{\frac{-t}{Z_o \cdot C_i}}$
Calibrator Load	$R_{eq} = \dfrac{Z_o \cdot R_M}{Z_o + R_M}$	Z_o
$V_{RM,cal}(t)$	$V_i \cdot e^{\frac{-t}{R_{eq} \cdot C_i}}$	$V_i \cdot (1 + \Gamma) \cdot e^{\frac{-t}{Z_o \cdot C_i}}$
$Q_{m,cal}$	$\dfrac{Z_o}{Z_o + R_M} \cdot q$	$\dfrac{2 \cdot Z_o}{Z_o + R_M} \cdot q$
$Q_{PD,inj}$	$\dfrac{1}{2} \cdot C_i \cdot V_i = \dfrac{q}{2}$	$\dfrac{1}{2} \cdot C_i \cdot V_i = \dfrac{q}{2}$
$Q_{m,PDevent}$	$\dfrac{Z_o}{Z_o + R_M} \cdot q$	$\dfrac{Z_o}{Z_o + R_M} \cdot q$
PD Reading	q	$\dfrac{q}{2}$

where:

$V_{cal}(t)$ = PD calibrator output voltage (V)
$V_{RM,cal}(t)$ = R_M voltage at calibration (V)
$Q_{m,cal}$ = Q measured at calibration (C)
$Q_{PD,inj}$ = PD event injected charge in one cable direction (C)
$Q_{m,PDevent}$ = Q measured for PD event along the cable (C)
PD Reading = $Q_{m,PDevent}$ / $Q_{m,cal}$ (C)

The PD event charge splits into two pulses traveling in opposite direction but the measuring equipment only measures one of them, i.e. q/2. For near end calibration, the measuring equipment still measures *q/2* but displays *q* due to the calibration factor.

Far end calibration utilizes a reference pulse which has travelled along the cable; hence integrating the cable attenuation characteristics which is not the case for near end calibration.

This is probably one reason for previous standards and papers to require "that calibration in terms of charge be accomplished by injecting a known charge at the end of the cable remote from the detector" [7]. The latest IEC 60885-3 standard requires now near end calibration in case of long cables without termination. Table 1 is therefore very useful to compare PD measurement results. Issues and discussions will mostly arise for long cable lengths in comparison of the measurement BW.

4 OPTIMIZED SETUP AND PROCESSING

4.1 Coupling Capacitor Model – Matching R_M to C_k

Their physical extension (1 m or more) indicates that coupling capacitors be modeled as a transmission line. We can consider the characteristic impedance to be close to 300 Ω (usual impedance of a connection wire in high-voltage impulse applications). This model leads to

matching R_M with the 300 Ω impedance of the capacitor instead of the characteristic impedance of the cable.

Simulation in Figure 5 compares full response and 20 MHz limited BW for R_M = 30 Ω and R_M = 300 Ω. A 10 ns propagation delay is used to represent the typical height of a 2 m coupling capacitor, filtering should already be below 20 MHz to avoid oscillations and distortions of the measured PD pulse.
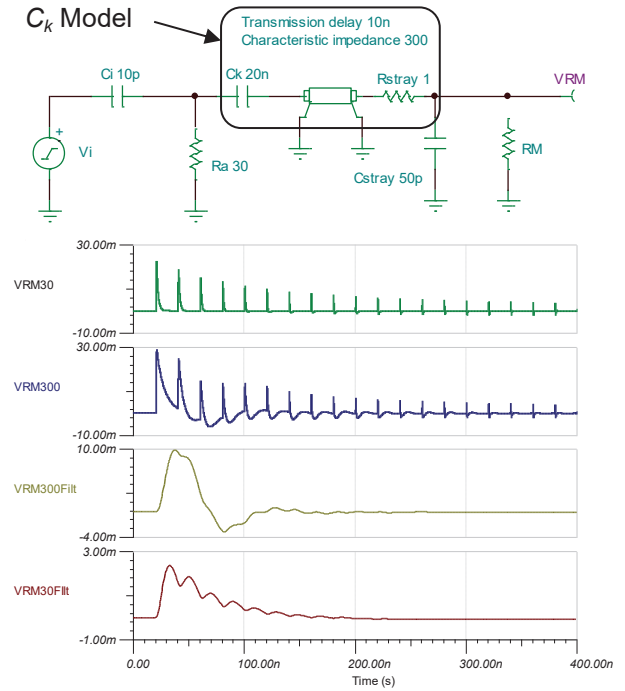

Figure 5: Modeling and simulation of the coupling capacitor C_k.

4.2 Matched Filtering

A matched filter is a filter which optimizes the signal-to-noise ratio of the filtered signal. The samples of a reference pulse shape h(n) of duration T reversed in time directly serve as the filter coefficients as expressed in Equation 9. The filter output is maximized when the signal correlates with the reference pulse.

$$H(i) = h(T - i) \quad 0 \leq i \leq T \qquad (9)$$

For cable fault location, the reference pulse can be recorded during PD calibration. Assuming the PD calibrator connection leads are kept shorter than the expected length/time resolution and the injection capacitance is small enough in comparison to other stray elements connected at the cable end, the pulse will almost have the same shape as a single PD event. The shape is close to the real PD event including the attenuation and BW limitation of the overall system. Calibration can be performed at a higher discharge level or signal

averaging can be applied to ensure that the reference pulse is noise-free.

The calibrator pulse must be short enough (i.e. C_i small enough) such that the BW of the calibration pulse is larger than the available bandwidth of the system. BW limitation is necessary because the cable itself has a limited bandwidth. Noise in the higher frequency range is more likely to enter the measuring system because the coupling capacitor and the circuit wiring both act as antenna. Fault location at cable ends requires to detect and eventually separate superimposed pulses.

4.3 Pulse Width Measurement

The pulse width can be measured from the matched filtered signal using the difference between two positive and negative maxima of the derivative. This method requires low processing power and is, in our example, almost as accurate as measuring the full width at half maximum (FWHM) of the auto-correlation of the pulse [7].
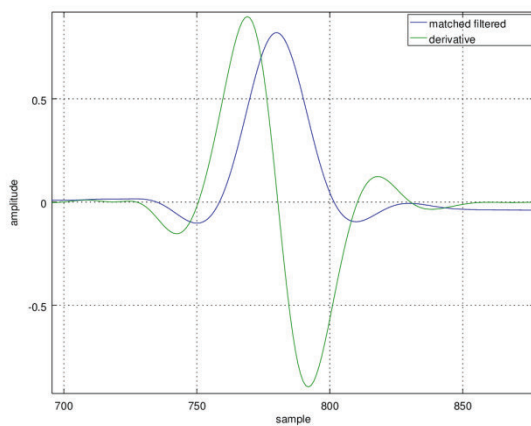
Figure 6: Pulse width derived from derivative

Whatever method is used for the pulse width measurement, the pulse shape is the very limiting factor. The width of superimposed ideal exponential pulses as shown in Figure 3, can be measured with the matched filtered/derivative method from 1 sample delay. The sharp peaks are even more visible after matched filtering.

For far end calibration, the recorded reference pulse has a limited BW and is very smooth at the peak value. As a result, the pulse width measurement is almost identical for superimposed pulses up to a shift of ten samples (one sample each 10 ns, which is equivalent to one meter in this example) as shown in Figure 7. This implies that for this case it is impossible to clearly distinguish and hence detect PD pulses originating from faults less than 10m from the far end. The same limitation is observed for the auto-correlation method. The graph from Figure 7 allows to assess the minimum pulse separation of the overall system, just by recording the calibration pulse.
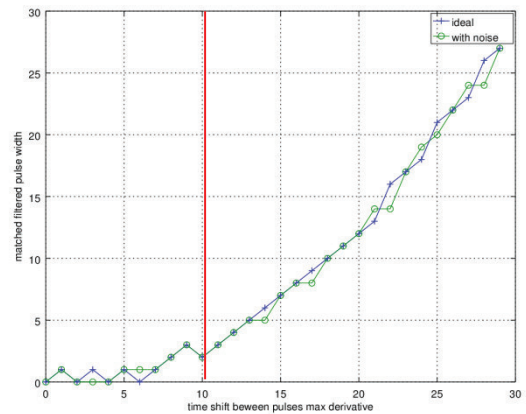

Figure 7: Detectable pulse resolution for far end calibration.

5 CABLE FACTORY TEST

The figures in the present section are based on cable factory test data for a 12/20 kV XLPE cable. Figure 8 shows the PD detector measurement using the time between the first and second peak, the cable fault location is calculated at 5 m.
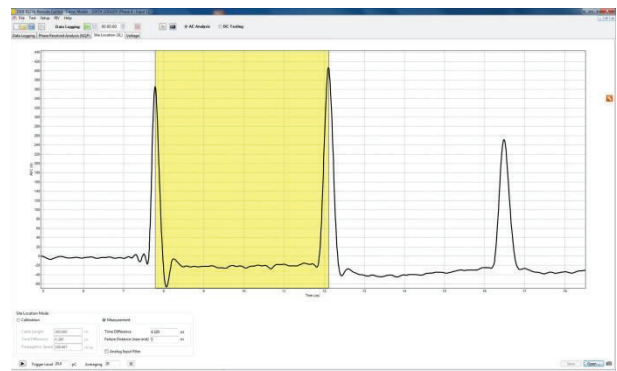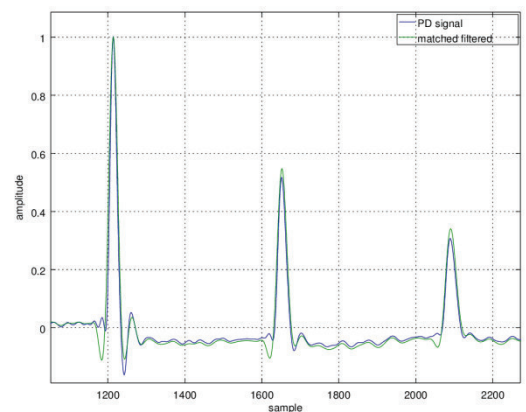

Figure 8: PD measurement, near end fault.

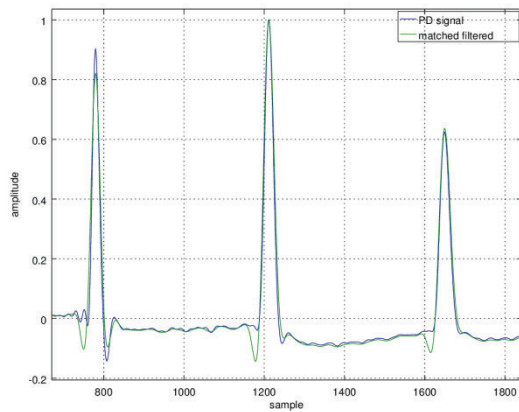**Figure 9:** Far end calibration post processing.

Figure 10: Near end fault PD post-processing.

Figure 9 and Figure 10 display post-processed calibration and measurement data using matched filtering. When using the matched filtered pulse, the distance between pulse #1 and #2 is increased to 7 m. The real fault was located at approx. 8 m.

6   RECOGNITION OF SUPERIMPOSED PULSES

When the time between pulses #1-#2 and #2-#3 is close to the propagation time of a single cable length, this is an indication for superimposed pulses. The magnitude pattern shown in Figure 11 can give some hints to the location of the fault.
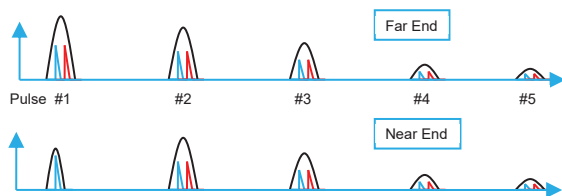

Figure 11: Near and far end patterns.

Case 1) The first pulse is lower than the second pulse. In that case, the fault is most probably at the near end.

Case 2) The first pulse is higher than the second pulse. In that case, the fault is most probably at the far end.

Case 1) can also occur for far end failures, which depends on how the superimposed pulses combine and are being reflected at the cable end. An open far end always has some stray capacitance and stub caused by removing the cable shielding. This means that the termination cannot be considered as an ideal open circuit. It is a complex impedance, unmatched stub with either negative or positive reflection coefficients depending on the signal frequency.

The ratio between measured pulse and far end calibration pulse can be used to distinguish a near end fault when:

- the ratio of the first pulse is < 1
- the ratio of the 2nd pulse is $\geq$ 1
- the ratio of the 3rd pulse is $\geq$ 1

7   CONCLUSION

To verify the detection method, we have used a 200 m RG-58 coaxial cable and we have simulated faults at 2, 3 and 5 m with an SMA connector directly coupling to the inner conductor. The near end fault was correctly located in all of the three cases. For the far end the fault distance could not be exactly determined but the correct cable end was identified in all cases.

We have covered the influence of measuring impedance R_M, coupling capacitor C_k and near or far end calibration on cable fault location measurements. This reveals R_M should be close to the coupling capacitor characteristic impedance, calibration should be performed at far end. The cable model for calibration is a resistor $R_a = Z_o$ which comes in parallel with R_M in case of near end calibration.

The time between pulses can be measured even in case of superimposed pulses. Matched filtering allows to reduce noise in an optimal way and to correctly detect the pulse position to measure time differences. The PD pulse shape determines the limits of pulse width measurements.

REFERENCES

[1] C. Knapp et al., "Signal Processing Techniques for Partial Discharge Site Location in Shielded Cables", IEEE Transactions on Power Delivery, Vol 5, No 2, April 1990.
[2] S. Boggs, "The Case for Frequency Domain PD Testing in the Context of Distribution Cable", IEEE Electrical Insulation Magazine, Vol 19, No 4, July/August 2003.
[3] IEEE Std 400.3-2006 , "IEEE Guide for Partial Discharge Testing of Shielded Power Cable Systems in a Field Environment", February 2007
[4] R. Anderson et al., "S-Parameter Techniques for Faster, More Accurate Network Design", Test & Measurement Application Note 95-1, Hewlett Packard, 1997.
[5] P. Treyer et al., "Breaking the Limit of Power Capacitor Resonance Frequency with Help of PD Pulse Spectrum to Check and Setup PD Measurement, ISH Pilsen, August 2015.
[6] P. Treyer et al., "Innovative Application of Frequency Response Analysis for Partial Discharge Measurement", ISH Pilsen, August 2015
[7] S. Boggs, G. Stone, "Fundamental Limitations in the Measurement of Corona and Partial Discharge", IEEE Transactions on Electrical Insulation, Vol 7, No 2, April 1982.

Global Presence

Europe
HAEFELY AG
Birsstrasse 300
4052 Basel
Switzerland

☎ + 41 61 373 4111
✉ sales@haefely.com

China
HAEFELY AG Representative Office
8-1-602, Fortune Street, No. 67
Chaoyang Road, Beijing 100025
China

☎ + 86 10 8578 8099
✉ sales@haefely.com.cn

HAEFELY
Current and voltage – our passion

HV HIGH VOLTAGE

I INSTRUMENTS

E EMC